2019 IEEE 39th International Conference on Distributed Computing Systems (ICDCS)

CBMA: Coded-Backscatter Multiple Access

Nanhuan Mi*‡, Xiaoxue Zhang*‡, Xin He*‡, Jie Xiong†, Mingjun Xiao‡, Xiang-Yang Li*‡ and Panlong Yang*‡
‡University of Science and Technology of China (USTC), *USTC LINKE Lab, †University of Massachusetts Amherst
Email: {nhmi95, zxx97}@mail.ustc.edu.cn, {aaronhexin, xiangyang.li, panlongyang}@gmail.com,
jxiong@cs.umass.edu, xiaomj@ustc.edu.cn

***Abstract*—The ever-increasing number of IoT devices in our surrounding environment bring us tremendous amount of opportunities but also challenges including limited battery life, low computational capability and scalability of multiple access. Recent advances in backscatter communication have enabled ubiquitous IoT devices to communicate in a cost- and power-efficient way. However, most of the proposed backscatter solutions nowadays focus on the single tag paradigm, *i.e.*, multiple tags do not transmit simultaneously and thus the solutions have difficulties to scale with a large number of tags.**

This work presents CBMA, a backscatter system that enables multiple concurrent backscatter tags to communicate reliably and efficiently. For the first time, we demonstrate that multiple tags can backscatter concurrently and efficiently with novel impedance-based power control at the tag, and can be successfully decoded with commodity WiFi devices without affecting the existing WiFi communication. We present the design details of CBMA and build a prototype with off-the-shelf WiFi devices and FPGA. The CBMA system achieves a 10-tag bit rate of 8Mbps while supporting a communication distance up to 10m. Compared to single-tag solutions, CBMA improves the backscatter throughput by more than 10× even in challenging indoor scenarios with rich multipath and interference.

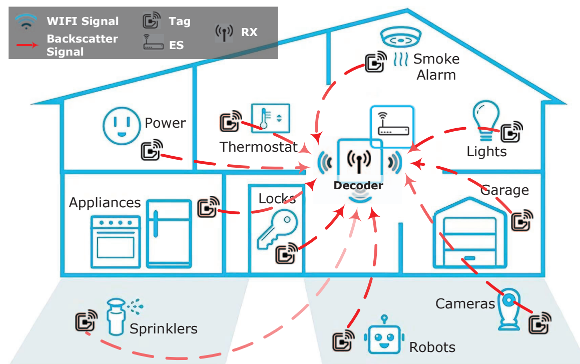

Fig. 1: A typical application scenario of the CBMA backscatter system.

I. Introduction

While traditional WiFi networks have achieved a great success in providing higher and higher transmission rates for each single device, the recent trend of more and more IoT devices brings in new requirements and challenges for future network design. By year 2020, 30 billions of IoT devices are expected and the number keeps increasing by 20% per year [1]. These huge amount of devices will be deployed around us or even on our body to provide various types of sensing to improve the quality of our lives. Different from the traditional laptops and smartphones which require high transmission rates, the IoT devices usually transmit data at low rates or in a burst manner. Another challenge is the tiny power budget for these IoT devices without power plug. Recently, backscatter communication has attracted a lot of attention owing to its low-power and easy-to-deploy nature. With backscatter technologies, the low power requirement has mostly been met. However, in the framework of backscatter communication, the existing works focus on single node (tag) scenario and multiple tags still have difficulties to communicate simultaneously, severely limiting the scalability to accommodate large number of IoT devices, *e.g.*, smart home in Figure 1.

To enable efficient and scalable backscatter communication, the following two issues should be addressed.

- *Capacity.* Since the number of devices is huge, the backscatter communication should offer high capacity to not just a single node but as many nodes as possible simultaneously. *i.e.*, an appropriate multiple access scheme is indeed required.
- *Control.* It is extremely difficult to achieve centralized control for networks with a huge number of nodes, and hence the backscatter communication should be conducted in a distributed manner.

To realize high capacity, current approaches are built based on anti-collision schemes, which mainly include two multiplexing technologies: frequency-division multiple-access (FDMA) and time-division multiple-access (TDMA). In FDMA, different tags are assigned different frequency channels to communicate with the receiver. The tag should be capable to freely adjust the transmission frequency within the bandwidth. In this case, the cost of the tag is increased and the receiver should work as a control node to assign the frequency band. Furthermore, the available bandwidth is extremely limited, which results in FDMA being a much expensive solution for large scale deployment. TDMA is the most popular multiplexing method for backscatter technology. The medium access schemes can be either deterministic, typically tree-search based schemes, or probabilistic, *e.g.* framed slotted ALOHA (FSA)-based schemes. However, the receiver acts as the centralized control node in FSA, which coordinates the frame size in the network. Therefore, FSA fails to meet the distributed manner requirement.

To the best of our knowledge, the existing backscatter systems rarely take into account both the requirements (see Table I). BackFi [2] focuses on improving the data rate in

2575-8411/19/$31.00 ©2019 IEEE
DOI 10.1109/ICDCS.2019.00084

TABLE I: Summary of existing backscatter systems.

Technology	Data Rates (bps)	Number of Tags	Distance (m)
Ambient Backscatter	1kbps	2	$\leq$ 1m
Wi-Fi Backscatter	1kbps	1	0.65m
BackFi	5Mbps	1	1m
FM Backscatter	3.2kbps	1	18m
LoRa Backscatter	8.7bps	1-2	475m
PLoRa	6.25kbps	1	1.1km
Netscatter	500kbps	256	2m

a range up to 1m. FM Backscatter [3], LoRa backscatter [4] and PLoRa [5] enable long-range backscatter communication, however, they do not consider multiple access and high data rate. Netscatter [6] deploys a large amount of tags with a limited data rate and/or short communication range. In addition, how to adopt decentralized control on the tags is lack of discussion in these works.

Instead, this paper proposes a coded-backscatter multiple-access (CBMA) scheme for backscatter communication to meet both the requirements, inspired by direct sequence spread spectrum (DSSS). DSSS is resistant to fading and shows strong capability to support simultaneous transmissions from multiple tags. However, to design and implement the CBMA scheme in backscatter, we face the following challenges:

- **Asynchronous signal.** It is difficult to coordinate all the tags by sending a controlling signal, which leads to asynchronous transmissions from tags. The orthogonality of the spread sequences is significantly affected by the asynchronous problem, and thus conventional approaches are inappropriate to separate the signals.
- **Diverse received power.** The strength of the backscatter signal is essentially weak and strongly affected by the distance between the tag and the receiver. The received signal strength thereby varies among the tags which causes significant performance degradation due to the well-known near-far problem [7] in conventional code-division multiple-access (CDMA) systems. What makes the problem even more challenging is that the power control is extremely difficult at the tag since the tag does not generate RF signal directly by itself.

To address these two challenges, we propose two schemes in the framework of CBMA: 1) correlation-based detector and 2) power control at the tag. The correlation-based detector aims to reduce the negative effects caused by the asynchronous problem, while the purpose of the power control scheme is to improve the performance against the significant power difference among tags. To our best knowledge, this work is the first one to enable power control at the passive tag side by changing the tag antenna impedance. Furthermore, we build a prototype of CBMA using two USRP RIO devices and several customized tags with FPGA implementation. In summary, our proposed multi-access system exhibits the following favorable properties:

- **Robust transmission**. Due to the weak strength in backscatter signal, robustness is one of the most important features that a multiple-access system needs to bear.
- **Design efficiency**. The overhead is small both in computational domain and communication domain. The tag only needs to perform AND operation to spread its signal.
- **Power control**. In our design, the tags can auto-adjust their impedance to improve overall performance.

Contributions. We make the following contributions:

- CBMA is the first design in advocating simultaneous tag backscatter transmissions with CDMA scheme. We demonstrate that multiple tags can backscatter information concurrently using the proposed approaches with very little overhead, and the content can be decoded by commodity WiFi NICs without affecting the original WiFi communication. We have verified the performance with testbed experiments for 10 tags.
- CBMA presents the first power control scheme at passive tags with hardware implementation. It tunes the impedance of the tag antenna to control the power for more efficient backscatter. Furthermore, a node selection method is proposed upon this design to improve the capacity by realizing the adaptive multiplexing scheme.
- We build a prototype of the CBMA with off-the-shelf hardwares. It achieves a multi-tag bit rate up to 8Mbps with tag-receiver distances up to 5m. Compared to single-node solutions, CBMA can improve backscatter throughput by more than 10$\times$ in challenging indoor scenarios with obstacles and interferences.

The rest of this paper is organized as follows. The preliminary knowledge on backscatter communication and multiple access is given in Section II. The system overview of CBMA is presented in Section III. In Section IV, we provide a measurement for demonstrating why power control is required. We describe the detailed design of CBMA in Section V. The implementation of CBMA-based backscatter system is stated in Section VI, followed by the evaluation results in Section VII. We give some discussions in Section VIII. Finally, the paper is concluded in Section IX with several remarks.

II. Preliminaries

A. Backscatter communication systems

A typical backscatter communication system consists of a transmitter (usually referred to as an excitation source), a group of tags and a receiver. The backscatter tag reflects and modulates the incoming excitation signal to transmit its information to the receiver.

Excitation source: It sends out a single-frequency tone or other signals (*e.g.*, WiFi, Bluetooth) as the excitation signal in the backscattering system, and serves as a power charging infrastructure for the tag. The tone signal can be simply represented as $\sin(2\pi f_c t)$.

Backscatter tag: The backscatter tag is composed of an antenna, a receiving module and an FPGA-controller which controls the single pole double throw (SPDT) switches to choose different resistances to generate backscattered signals. By changing the impedance of the antenna, the tag can control the amount of backscattered power. In practice, we use a square wave at frequency of Δf to control the antenna impedance, and the resulting frequency is $f_c - \Delta f$ and $f_c + \Delta f$.

Receiver: A receiver node tunes its center frequency to one of the shifted signals, which is $f_c - \Delta f$ in our configuration. As described above, the received signal is generated by modulating the tone signal from the excitation source using the square wave of backscattering tag in the air.

B. Multiple access of backscatter communication

In conventional backscatter communication, the case that multiple tags backscatter information at the same time in the same frequency band is rarely considered. However, the design of multiple-tag backscatter communication is extremely important in dense IoT systems. Due to the limited capability of the tag (there is no ADC on the tag so that the strength of signal is unknown), it is infeasible to carry out carrier sense at the tag side, which leads to a completely different situation compared to the conventional multi-user communication. Typically, in backscatter communication, several methods can be applied to avoid collisions among tags.

CDMA-based multiple access is one of them. In this scheme, each tag has a local "pseudo-noise" (PN) code to spread its information. The PN code is referred to as "pseudo-random" for the reason that the code is predictable and repetitive, although it appears to be random noise. At the tag, each bit of the information is multiplied by the PN code, which is independent of the information, to produce a coded sequence being backscattered. At the receiver, the original data is reconstructed by multiplying the received data with the same PN code. Owing to the orthogonality properties among PN codes, the interference from the sequence with a different PN code is minimized. Therefore, multiple access is achieved by using different PN codes at different tags.

C. PN sequence

A PN code is a binary sequence that appears randomly but can be reproduced in a deterministic manner by intended receivers. These PN codes are used to encode and decode a user's signal in asynchronous CDMA in the same manner as the orthogonal codes in synchronous CDMA. These PN sequences are statistically uncorrelated, and the sum of a large number of PN sequences induces multiple access interference (MAI) that is approximated by a Gaussian white noise. If all users are received with the same power level, then the amplitude (*e.g.* the noise power) of the MAI increases in direct proportion to the number of users. In other words, unlike synchronous CDMA, the signals from other users will appear as noise with respect to the signal of interest and interfere slightly with the desired signal in proportion to the number of users.

III. CBMA Overview

CBMA system consists of an excitation source, N tags and a receiver. The excitation source (ES) broadcasts a tone signal or orthogonal frequency-division multiplexing (OFDM) signal to serve as the excitation signal and powering source of the backscatter system. Each tag spreads its information using a specific PN sequence, which is different with other tags, and conveys the spread information by reflecting and modulating the excitation signal. The receiver then performs a series of operations to decode the received signal. The structures of the tag and the receiver are shown in Figure 2.

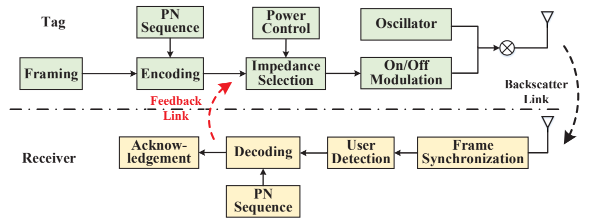

Fig. 2: The structure of the tag and the receiver of CBMA backscatter system.

A. Backscatter Tag

The backscatter tag in the CBMA system performs the following operations, including framing, encoding, power selection, upsampling and frequency shifting processes.

Framing. The data of the tag being transmitted is first encapsulated to frames with the following fields: (1) one byte known preamble $\{10101010\}$; (2) one byte data indicating the length of the frame; (3) up to 126 bytes of payload data and (4) two bytes of cyclic redundancy check to verify whether error has occurred.

Encoding. The structured frame is then processed by the encoding block using a PN code which is deterministically generated at the tag. The data is then multiplied by the PN code. Here, we give a simple example to illustrate the encoding process. Assume that the tag wants to transmit "10" and a PN code "01001" is adopted, the result of encoded data is then "0100110110". In this work, two types of PN codes are considered, which are Gold code [8] and 2NC code [9].

Power control. The system performance is significantly affected by the received power level from each tag. Based on the principle of traditional CDMA system, the best case is that the received power from each tag is kept at the same level. Hence, power control is extremely critical for CDMA system. It is found that the strength of backscatter signal highly depends on the impedance of the tag antenna, and thus the backscatter power could be adjusted by changing the impedance. We propose an effective power selection algorithm by adaptively adjusting the impedance of the tag antenna to optimize the overall system capacity.

On/Off modulation and frequency shifting. The coded sequence using the specific PN code is then employed to perform On/Off modulation on the backscatter signal. Since there is no RF front end for the tag to modulate its data, a square wave generated by an oscillator is used to control the reflecting state of antenna. The square wave could modulate with the excitation signal, leading to a frequency shifted backscatter signal. If the tag wants to transmit '1'/'0', it enables/disables

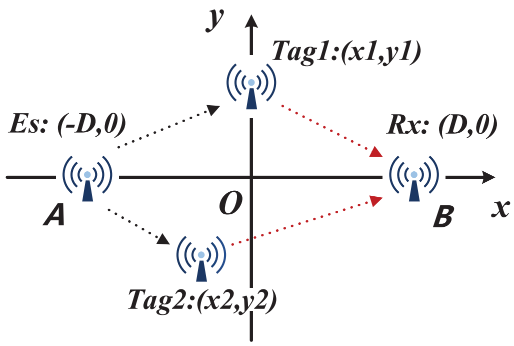

Fig. 3: The experiment scenario of benchmark experiments to evaluate the impact of power difference on the error rate.

the square wave to control the state of antenna for a period of one symbol time ($1\mu s$ in our configuration). Thus, we achieve On/Off modulation without an RF front end.

B. Receiver

The receiver listens to the channel with the central frequency which is the shifted frequency. If the data frame is detected, the receiver takes the samples with a sampling frequency f_s and initiates the receiving process, including frame synchronization, user detection, decoding and acknowledgement.

Frame synchronization. The frame synchronization is achieved by energy detection with a sliding window. Concretely, a moving average filter is first performed on the received energy level with a window size W_n. The filtered sequence is then passed through a comparator to determine whether a new frame is received by comparing the current power level and the filtered power level. We use a decision threshold P_{th}, which is configured as 3dB higher than that of filtered power level.

User detection. To decode the incoming frame, it is necessary to determine which PN sequence is included in the frame. We utilize the orthogonality feature among PN sequences to perform user detection. Specifically, we use each of the PN sequences to cross-correlate with the preamble of the received frame. If the correlation value of a PN sequence is larger than a predetermined threshold, the user with this PN sequence is determined to be in the frame with high probability.

Decoding. After user detection, we use the PN sequences of the detected users to perform cross-correlation with each chip (the spread symbols to represent one bit) from the synchronized frame. If the correlation with the PN sequence representing '1' is higher than that with the PN sequence representing '0', the chip is decoded to '1', and vice versa.

Acknowledgement. The receiver broadcasts the acknowledgement message to the backscatter tags to indicate the ID of the successfully decoded tags. For example, the information from tag 1 and tag 3 are correctly decoded, the receiver then sends an ACK message that shows tag 1 and 3 are decoded. The ACK message is very important for the tag to adapt the power level, which is detailed in Section V.

TABLE II: Error Rate vs the power difference.

Case	SNR1 (dB)	SNR2 (dB)	Difference	Error Rate
1,2	7.9	4.1	58.06%	19.25%
1,3	4.5	4.8	6.67%	**0.47%**
2,3	3.1	3.4	9.09%	**0.85%**
1,4	5.3	8.3	50.00%	16.36%
3,4	6.6	6.6	0.00%	**0.32%**
2,4	10.5	5.6	68.42%	38.07%
2,5	8.4	8.4	0.00%	**0.21%**
4,5	6.0	5.7	5.00%	**0.38%**
1,5	5.6	9.1	56.10%	15.98%
3,5	8.6	3.0	26.00%	21.36%

IV. Verification of the Effect of Power Difference Between Tags

The challenge for collision decoding in practical backscatter systems mainly lies in different power of tags. Theoretically, when several tags collide, we can decode the data of each tag by cross-correlation if the power of tags are linearly combined. However, we observe a poor decoding performance when the tags have a big power difference between each other. Thus, it presents a conundrum that: how to address the large power difference between tags? Our idea is to tune the tag antenna impedance to control the backscattered power. We then conduct benchmark experiments in a two-tag collision case. We build a coordinate system as shown in Figure 3. The points marked A and B indicate the excitation source 'Es' and the receiver 'Rx'. The point marked O is the origin of this coordinate system. We then place the excitation source and the receiver at position $(-D, 0)$ and $(D, 0)$ respectively ($D = 50cm$ in our implementation). Meanwhile, we denote (x_1, y_1) and (x_2, y_2) as the position of '$Tag1$' and '$Tag2$' in one test. For each test, we choose two of the five tags (indicated by 1, 2, 3, 4 and 5 in Table II) and randomly place them. Under the limitation of the space, we only present parts of the results in Table II. The difference is calculated as the ratio between the power difference and the larger power of the two. And the error rate is calculated as the number of missing packets over the total number of transmitted packets. We find that when the power difference is below 10% (the power of two tags are similar), the error rate is much lower. Consequently, we can leverage these results to carry out power control to improve throughout performance. We propose our power control scheme and present the details in the following section.

V. Design of CBMA

In this section, we present the detailed design of the CBMA backscatter system, including the power control and the node selection schemes.

A. Communication on Tags

As stated in Section III, if the tag wants to transmit '1', it enables the square wave to control the state of antenna for one period of symbol time. Otherwise, the tag keeps silent and

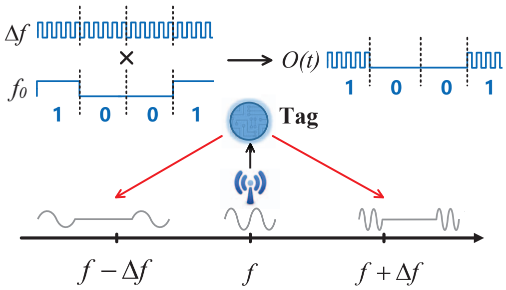

Fig. 4: The schematic diagram of the modulations carried out at the tag. Let a square wave at a frequency of Δf be modulated with data packet at a bit rate of f_0, which is generated by the micro-controller and used to control the impedance of the antenna. So the frequency shifts of generated narrow band signals are $f - \Delta f$ and $f + \Delta f$.

does nothing. Specifically, we have a two-layer modulation to achieve our backscatter communication on tags. The first one is to generate Δf frequency shift by sending a square wave as mentioned in the previous section. The other on-off key (OOK) modulation is to transmit data bits with tags. In this modulation, the square wave serves as carrier wave. The presence of the carrier for a specific duration represents a binary '1', while its absence for the same duration represents a binary '0'. Consequently, at the receiver side, receiving signal can be decoded as '1', and none signal can be decoded as '0'. In practice, we execute an 'AND' operation of the square wave and data flow after upsampling as shown in Figure 4[1]. To change the bit rate, the only thing to change is the time period of tag reflecting (ON) and absorbing signals (OFF).

B. Impedance Selection

Power Control Scheme: We receive the backscatter signal in I-Q space: $I(t)$ and $Q(t)$. The power of received signal is $P(t) = \sqrt{(I^2(t) + Q^2(t))}$. As our sampling rate is higher than the bit rate, we downsample the received data first. Each tag has its own PN code. When the receiver detects a preamble for a tag, it sends an ACK packet back to this tag. As a result, when the tag receives few ACK feedback packets, we consider that most of transmitted packets through this tag are lost. The reason is that the power of the backscattered signal is too low to be detected by the receiver. To improve the transmission performance, we have to increase the power. As mentioned above, we can change the antenna impedance to tune the reflection coefficient Γ^* to achieve power control. We present the pseudo code of the power control algorithm in Algorithm 1 and we omit the downsampling and decoding processes. In our experiment, the power control is performed circularly to try every possible power level. To avoid our power control scheme to fall into an infinite loop, we limit the number of execution cycles to 3 times the number of tags.

Algorithm 1: Power Control

Input: Received Signal I, Q, Data: M
Output: Adjusting impedance(Z) strategy

$P \leftarrow (I^2 + Q^2)^{\frac{1}{2}}$;
$Downsampling$;
$n \leftarrow numberoftags$;
$m \leftarrow numberofpackets$;
for $i = 1 \rightarrow n$ **do**
  $ACK_i \leftarrow 0$;
  while *there is data* **do**
    if *preamble is detected* **then**
      $ACK_i = ACK_i + 1$;
    end
  end
  $ACKratio_i \leftarrow ACK_i/m$;
end
$FER = 1 - \sum_{i \in n} ACK_i/n$;
if $FER > Threshold$ **then**
  for $i = 1 \rightarrow n$ **do**
    if $ACKratio_i < 50\%$ **then**
      if $Z == Z_{max}$ **then**
        $Z \leftarrow 1$;
      else
        $Z \leftarrow Z + 1$;
      end
    end
  end
end
return Z;

C. Node Selection

However, even with the proposed power control scheme, some tags still cannot receive ACK messages and the error rate is still high. The reason is twofold. First, the backscatter signal is much weaker than the excitation signal. If some of the tags are quite far away from the receiver, their power becomes too weak to be detected at the receiver even if we set the tag power to the highest possible value by tuning the impedance. Second, when two tags are physically close to each other, they will interfere with each other, resulting in poor system performance. Tuning the power level does not help much in these two cases.

To address the limitation of our power control scheme, we propose another optimization scheme for node selection. If the system performance cannot meet the expectation with power control, we abandon those 'bad' tags whose successful ACK feedback rate is below 70%. Therefore, the main question is how to reselect the tags. In our system, the communication range depends on two factors: (i) the distance between the excitation source and the tag and (ii) the distance between the tag and the receiver. Specifically, the signal strength at the receiver, P_r, can be represented using Friis path loss model as follows

$$P_r = (\frac{P_t G_t}{4\pi d_1^2})(\frac{\lambda^2 G_{tag}^2}{4\pi}\frac{|\Delta\Gamma|^2}{4}\alpha)(\frac{1}{4\pi d_2^2}\frac{\lambda^2 G_r}{4\pi}). \quad (1)$$

This equation has three key parts: the term in the first parenthesis models signal propagation from the excitation source (signal transmitter), with a transmission power P_t and

[1]For simplicity, we do not examine the effect the double sideband caused by the frequency shift using a square wave. In fact, we can use the method proposed in [10] to generate single sideband backscatter signal.

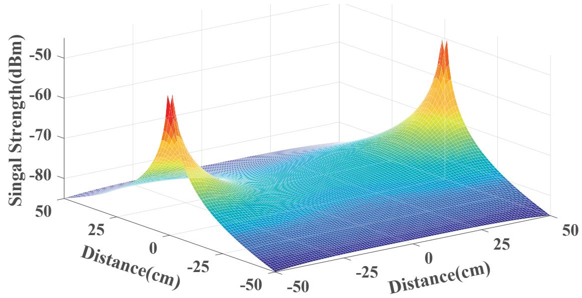

Fig. 5: Theoretical results of backscatter signal strength.

an antenna gain G_t, to a tag at a distance d_1 away. The third term, similarly, models the signal propagation from the tag to the receiver with an antenna gain G_r at a distance d_2. Here, λ is the wavelength of the signal transmitted. The term in the middle parenthesis models the fraction of incident signal from the excitation source that is backscattered by a tag with an antenna gain G_{tag}. $|\Delta\Gamma|$ is the backscatter coefficient. According to this equation, we can obtain theoretical results of the received signal strength at each position as Figure 5 shows. Our node-selection method is a greedy algorithm which continually moves at the direction with increasing received signal strength to select a tag with higher P_r.

When there are many tags distributed in the environment, we choose some of them in a group to transmit data. We abandon a 'bad' tag after power control in each round. We first randomly select an idle tag, and then calculate the difference of the theoretical received signal strength of original tag and this new one. If the difference is less than 0, we replace the old one by this new one. However, in order to avoid the situation that the selected tags in one group is concentrated, once a tag is selected, we exclude those tags near to this selected tag for consideration. We pick one tag randomly. If the new tag improves the received signal strength, it is always accepted. Otherwise, we accept the new tag with a probability less than 1. This probability decreases as time T goes up: worse positions are more likely to be allowed at the start when T is small, and they become more unlikely as T increases. Besides, when there are not enough tags to choose from in the environment, we have to change the positions of those 'bad' tags to improve system performance.

VI. Implementation

We implement a prototype of our system using commodity WiFi transmitter, designed backscatter tags and a USRP receiver. The equipments are shown in Figure 6. We describe the implementation details below.

Excitation source and receiver implementation: Our receiver is implemented on the latest USRP RIO platform with the LabVIEW Communications System Design Suite.

Tag implementation: We now describe the implementation details of our backscatter tag. The prototype of our tag is a customized design of passive tag, which backscatters the signal of the excitation source to the receiver. Our tag design

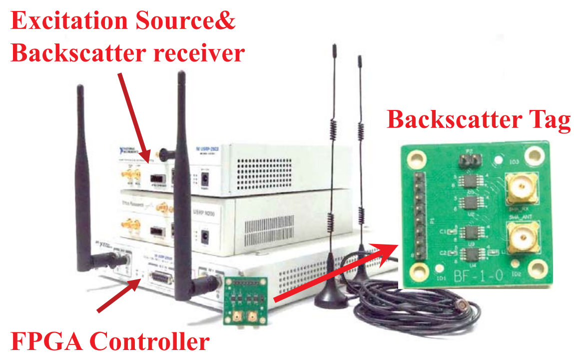

Fig. 6: Equipments used in our experiments.

is implemented as a Printed Circuit Board (PCB), whose main components are SPDT switches, antenna interfaces, pins and multiple different resistors. The size of the PCB is about $2.5 \times 2.5cm^2$. We execute power control using these SPDT switches that switch among the four different impedances of the antenna. To make sure our board can work with high frequency signals, we choose the HMC190BMS8 SPDT [11]. The four components connected to the four terminals of the switch to create different amounts of impedances are a 3pF capacitor, a 1pF capacitor, open impedance, and a 2nH inductor. An additional FPGA is used to control the backscatter state of the passive tag. The reflected signal is received and processed by a NI USRP RIO platform. Signal reflection only consumes power in the scale of μW [12].

Our software platform is built upon the LabVIEW Communications System Design Suite, where the software design could be imported to our aforementioned hardware platform. First of all, we need a carrier signal entered at 2GHz. To create a frequency shift, which is 20MHz in our system, we generate a sine wave using the square waves. Our FPGA design is applied to produce the square wave. With Fourier analysis, a square wave can be written as:

$$Square(\Delta ft) = \frac{4}{\pi} \sum_{n=1,3,5\ldots}^{\infty} \frac{1}{n} \sin(2\pi \Delta ft). \tag{2}$$

Here the first harmonic is a sinusoidal signal at the desired frequency Δf. Note that the power of each harmonic decreases quickly in the scale of $\frac{1}{n^2}$. So the third and the fifth harmonics are about 9.5dB and 14dB lower than the first harmonic. Thus, we can approximate a square wave as the sinusoidal signal, that is $\frac{4}{\pi}\sin(2\pi\Delta ft)$. As mentioned in Section III, we apply OOK mudulation scheme to generate data on square wave. For our backscatter tag, we send data on frequency channel centred at f_0. We first upsample the data at $A(f_0 t)$ to the carrier frequency of Δf, that is $A'(\Delta ft)$. Then, we can operate on upsampled data and the square wave on Δf to generate synthesized signal $O(t)$ as below:

$$O(t) = A(\Delta ft)\sin(\Delta ft)$$
$$O(t) = \begin{cases} 0 & A(f_0 t) = 0 \\ \sin(\Delta ft) & A(f_0 t) = 1 \end{cases} \tag{3}$$

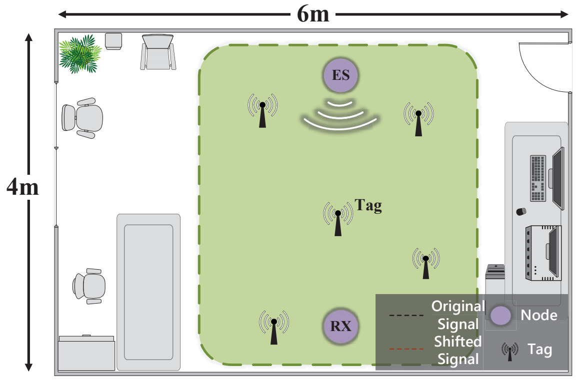

Fig. 7: The working environment of conducting measurements.

That is, when sending a bit '1', the tag generates square ware at central frequency Δf. Otherwise, the tag keeps silent and does nothing.

VII. Performance Evaluation

We describe the experimental evaluation of our system to understand how our system performs in various deployments.

A. Experiment Setup

We analyze the performance of our system in a typical office environment with a size of $4m \times 6m$. One USRP RIO serves as an excitation source for generating excitation signals and the other one serves as a receiver. USRP RIO can be replaced by commercial WiFi NICs in the experiment. The excitation source, the tags and the receiver are placed on a table as shown in Figure 7.

B. Micro Benchmark

1) Frame Detection: We first focus on the frame detection of our system. As a core component, it has a significant impact on the overall system performance. The frame detection is affected by many factors, including the distance, the transmission power of ES, the length of preamble and the bitrate. To evaluate the impact of these factors, we place an excitation source, a group of tags and a receiver in the office environment as shown in Figure 7.

Impact of distance. We first study how the error rate of frame detection changes with respect to the distance. In the experiments, we fix the ES-to-tag distance as 50cm and change the tag-to-RX distance from 10 to 400cm at a step size of 10cm. The number of tags in the experiments is set at 2, 3 and 4. In each case, we collect 1000 collided packets and measure the frame error rate (FER). The results are shown in Figure 8(a) and we can observe that: i) when the distance is greater than 2m, as the distance increases, the FER slightly increases. Compared to conventional wireless systems, this error rate is a bit high. This is because the strength of backscattered signal is much lower than conventional wireless signal; ii) when the distance is below 2m, the error rate almost keeps at a constant value, which depends on the number of tags. As expected, 2-tag case achieves the lowest FER among these experiments.

Impact of power. We then evaluate the performance of changing the backscatter power. However, it is challenging to directly change the backscatter power. We thus change the transmission power of the excitation source which is linearly related to the backscatter power. According to the Friis path loss equation, backscatter power and the excitation source power are linearly related to each other. Therefore, we evaluate the accuracy of frame detection with respect to the transmission power of ES. In the experiments, we vary the number of tags from 2 to 4, and the transmission power is changed from -5dBm to 20dBm at a step size of 5dBm. We collect 1000 collided packets for each setting and show the corresponding error rate in Figure 8(b). We find that as transmission power increases, the error rate decreases. When the transmission power is lower than 0dBm, the backscatter signal is so weak and can easily be buried in the environmental noise. We can see in Figure 8(b) the error rate is very high when the transmission power is lowered to -5dBm.

Impact of preamble length. To study the effect of the length of the preamble, we configure the preamble length as 4, 8, 16, 32 and 64 bits. For each case, we conduct experiments with varying number of tags from 2 to 4. Figure 8(c) shows the error rate of frame detection. We can see that the preamble length significantly affects the frame error rate. As the preamble length increases, the error rate decreases. In the 4-tag collision case, when the preamble length is set as 64bits, the error rate can be below 1%.

Impact of bitrate. We then study the impact of bit rate on frame detection. Since the sampling capacity of the receiver is limited, when the tags transmit at a particularly high bitrate, dwell time at each signal state is short, which may lead to too few sampling points and affect the performance of frame detection. In the experiment, the number of tags varies from 2 to 4. In each case, the bit rate changes from 250Kbps to 5Mbps. The results are shown in Figure 9(a). We can see that although bit rate is a key factor affecting the frame error rate, our system still achieves a fairly decent performance when the bit rate is 5Mbps.

2) User Detection: Next, we evaluate the performance of user detection module in the CBMA system. To minimize the influence of the frame detection, we adopt the best parameters obtained in the above section. A group of 10 tags are deployed for backscattering data. For each case, we randomly select a part of tags to send their data. The receiver uses all the PN codes of the tags in the group to detect which tag is backscattering. We perform the experiment 1000 times and the results demonstrate that we can 99.9% correctly detect which tags are sending data.

3) Cross-correlation based decoding: We now focus on the performance of cross-correlation based decoding process. We come up with two methods to improve the performance of the decoding process employing different PN sequences and performing power control at the tags. In practice, different

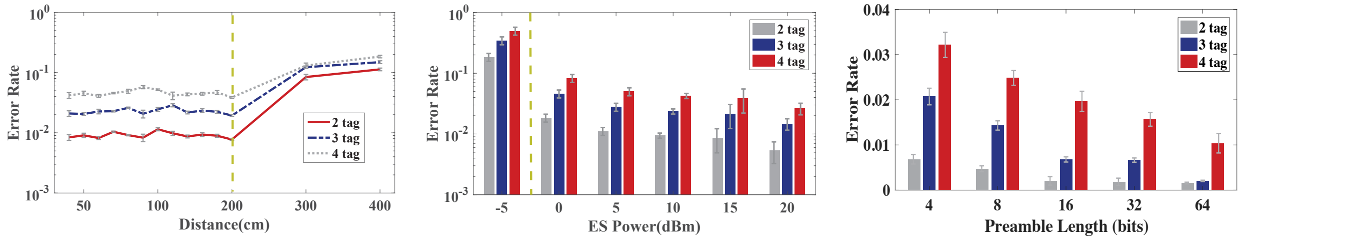

(a) Impact of distance.

(b) Impact of ES power.

(c) Impact of preamble length.

Fig. 8: The performance of evaluating the impact of different distance, ES power and preamble length.

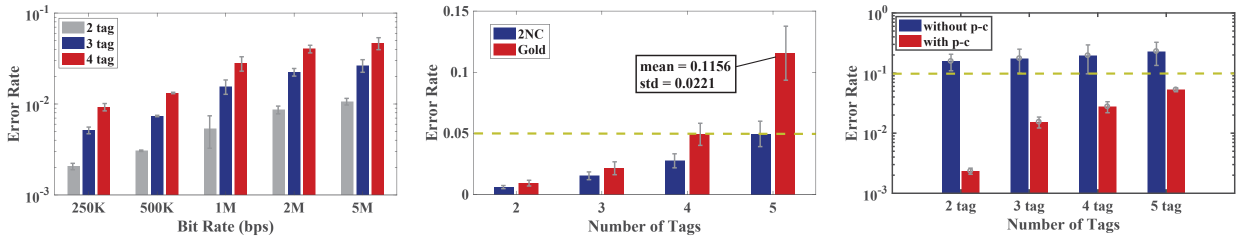

(a) Impact of bitrate.

(b) Impact of PN code.

(c) Impact of power control.

Fig. 9: The performance of evaluating the impact of different bitrate, PN code and power control.

PN codes have different auto-correlation and cross-correlation properties which can affect the performance of decoding. Moreover, as we have mentioned in Section VI, when the received power strengths from tags are similar to each other (with less than 10% difference), the decoding performance is superior.

PN codes. In the experiment, we test two types of PN codes: 2NC codes[2] and Gold codes. We change the number of concurrent tags from 2 to 5. Figure 9(b) demonstrates the comparison of the error rate for different adopted PN codes. It is found that as the number of tags increases, the error rate increases. Moreover, 2NC codes have better orthogonality which leads to less interference between tags, which means 2NC codes could achieve better performance. When Gold code is employed in 5-tag cases, the error rate suddenly rises up to 11%. We find that the performance of 2NC codes is better than Gold codes as expected. We thus adopt the 2NC codes in the following experiments.

Power Control. To analyze our power control scheme, we compare the performance of 2 to 5 tags, both with and without power control. For each setting, we generate 50 groups of random positions for tags. For each group, we evaluate the error rate of our system with power control and without power control, respectively.

Figure 9(c) illustrates the comparison on the error rate with and without power control. We find that without power control, error rate is much higher than that with power control. We can also see that with the number of tags increasing, the system error rate goes up. However, with power control, the system error rate is below 5% even when there are 5 tags. In the 5-tag collision case, the system performance is 5$\times$ better than that without power control.

[2]In our experiments, we modify the 2NC codes where the chip representing 0 is the negation of that representing 1.

C. Macro Benchmark

1) Deployment: To further investigate how the power control and tag selection schemes affect our system performance, we start with our experiments by placing several tags at random positions without power control. We randomly choose some tags to transmit data. Then we add power control module and finally we add the tag selection scheme. We plot the CDFs of error rate for the 5-tag case in Figure 10. The results clearly demonstrate the benefits of performing power control and tag selection. The performance with both tag selection and power control outperforms the other two cases.

Actually, it is difficult to achieve optimal performance only with power control. The reason is that at some positions, the power level of multiple tags cannot be tuned to be close to each other even with power control. Due to the random tag positions in real experiment, in some cases, the distance between the tag and the receiver is too large to achieve similar power level with power control. In addition, the distance between tags can be too small (smaller than half of wavelength). Then the interference between tags becomes large. We can see that, only with probability 0.6, the error rate is below 5% with power control. Therefore, we further adopt tag selection together with power control to improve the error rate performance.

2) Impact of Asynchronization: As the tags operate in a distributed manner, the backscatter signals from the tags may have time differences due to the different transmission delays, processing times, *etc.*. The impact of asynchronous receiving time on the system performance is studied. We set the number

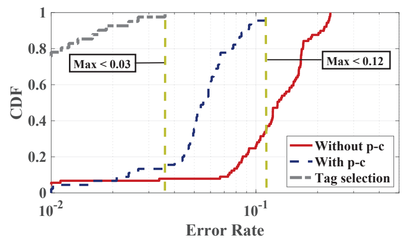

Fig. 10: CDFs of Error Rate.

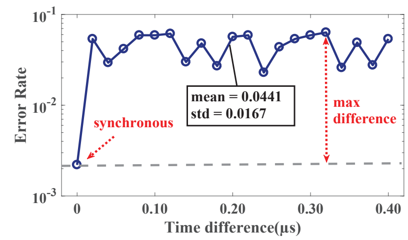

Fig. 11: Error Rate when tags are asynchronous.

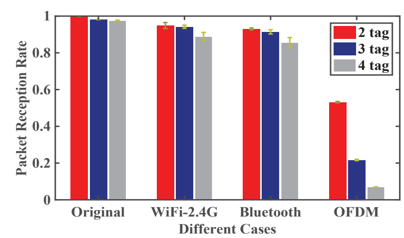

Fig. 12: Correct packet reception rate of system under different working conditions.

of tags as 2, and use the transmission clock of tag 1 as the reference. The error rate is evaluated by delaying the transmission clock of tag 2 with respect to the reference clock. As shown in Figure 11, the lowest error rate is achieved when the two tags are fully synchronized. The error rate dramatically goes up if there exists a time delay. The error rate fluctuates around 0.04 with a time delay.

3) Impact of Working Condition: This subsection evaluates the performance of our system under some "bad" working conditions. Figure 12 shows the impact of interference from the environment. The locations of tags are fixed. Four cases are compared: i) working without interference; ii) there are interfering WiFi signals in the environment; iii) there are interfering Bluetooth signals; iv) using OFDM signal as the excitation signal. We can see in Figure 12 that the correct packet reception rates for cases ii) and iii) are slightly lower than that for case i). The reason is that Bluetooth is based on frequency-hopping spread spectrum and WiFi transmission is based on CSMA/CA with random backup, so the channel is not always occupied. Therefore, interference from Bluetooth and WiFi transmissions are not severe. As a result, our system is robust and can coexist with commodity WiFi and Bluetooth with a negligible interference from them. However, when we use OFDM signals as excitation signals, the packet reception rate significantly drops. This is because OFDM signal is intermittent, and the tags do not know when there is signal they can reflect, leading to poor performance.

VIII. Discussions

A. Why not employ methods in frequency domain and spatio-temporal domain for multiple access?

Frequency domain methods need relatively complicated frequency sensing scheme and agile spectrum access method with high computational cost. It will bring in significant amount of latency and energy consumption at the backscatter tag side. On the other hand, for time domain methods to work, there is rigid timing requirement for synchronization. Maintaining a highly accurate timing control among passive tags needs new protocol design and the overhead will be non-negligible, over-complicating the tag design. There are indeed some opportunities in the spatial domain, because the system performance is highly dependent on the tag locations. The difficulty in leveraging this opportunity is the possible complexity in location information collection.

Our system incorporates the diversities and opportunities in code and spatial domain for efficient and reliable multiple access. It only needs a small amount of messages for cooperation, which is the node pair information. Compared with the FDMA and TDMA based methods, this overhead is much smaller and the design is lightweight.

B. Why employ the relatively inefficient CDMA scheme for efficient transmission?

The first reason is that the major concern for the backscatter multiple access is the interference. Weak backscatter signals are vulnerable to both intra-system interference, *i.e.*, reflections from other tags, and inter-system interference, *i.e.*, the ambient noise. CDMA based scheme is known to be robust against the aforementioned noises and thus works well with the backscatter system.

The second reason is we want a simple modulation scheme to achieve high throughput. Simplicity is particularly important for resource-constrained tags. The CDMA based scheme only needs simple XOR operations. Although the frequency spreading code makes the packets larger, the robustness achieved during the transmission makes this inefficiency negligible.

Finally, there may be other solutions to incorporate advanced modulation method such as OFDMA to enable multiple access. However, the high synchronization requirement and computational intensive FFT operations violate the fundamental rule of simple design for backscatter tags.

C. Why only 10 nodes are employed for testbed experiments?

The major reason is that we incorporate the FPGA design in our solution, which needs careful hardware design and additional time for manufacturing. Our hardware only has 10 pins so only 10 tags can be supported. Thus, we only include ten tags in our experiments. Note that, even in our emulation tests, we still utilize the real trace data delivered by the real field deployment tests, and incorporate the real imperfectness, *e.g.*, the timing error, in our emulation tests.

D. Starvation problem of the tag selection algorithm.

In the tag selection algorithm, we do not aim to select the tag with strong signal strength as "good" tag. Instead, we determine whether a tag is good by the overall performance of one group of tags. In particular, if the signal strength of the tags within a group are almost the same, the decoding performance will be notably good. Hence, the starvation problem can be probably solved by selecting different groups of tags. Furthermore, if the tag is moving, the starvation problem can be alleviated.

IX. Related Work

As an ultra low-power communication solution, backscatter communication recently has been attracted much attention [2], [9], [10], [12]–[24].

Motivated by the widely deployed wireless communication technologies, such as WiFi, Bluetooth, researchers focus on the design of backscatter communication with commercial radios. BackFi [2] enables high throughput backscatter communication with hardware modification by using ambient WiFi signals as excitation signal. WiFi backscatter [14] connects the RF-powerd devices based on backscatter communication. Passive Wi-Fi demonstrates that the tag can generate 802.11b backscatter packets [17] which is able to be decoded on any WiFi device. HitchHike [12] proposes a codeword translation to enable the backscatter communication using COTS WiFi transceivers, where it ensures the backscatter information is within the codebook of the WiFi signal by using the codeword translation technique. FreeRider [19] further extends the backscatter communication over other excited RF radios, such as Bluetooth, 802.11g/n WiFi and ZigBee. Reference [20] enables per-symbol and in-band backscatter communication using the residual channel knowledge of the WiFi packets. However, the multiple access control protocol has not been fully addressed in these work. There is only brief discussion rather than the detailed analysis in a part of these work, *e.g.*, FreeRider adopts FSA-based random access technique to avoid collision. Besides, the multiple access control is considered in backscatter-based RFID systems, *e.g.*, TDMA-based FSA [25], FDMA [26], CDMA [27], spatial division multiple access [28], and decoding collision [29], [30]. Netscatter [6] adopted chirp spread spectrum to enable multiple tags to simultaneously backscatter their information. This work analyzes the CBMA-based backscatter communication to enable the tag simultaneously transmits data to the receiver in the same frequency band.

X. Conclusion

CBMA enables up to 10 backscatter tags to concurrently backscatter data in a reliable and efficient way. For the first time, we demonstrate that multiple tags can transmit concurrently with simple power control scheme on tags, and can be decoded by commodity WiFi hardware, while keeping the original WiFi data communication unaffected.We present the design details of CBMA and build a prototype with FPGAs and off-the-shelf WiFi devices. The CBMA system achieves a multi-tag bit-rate up to 8 Mbps with tag-receiver distances up to 5 m. Compared to single-tag solutions, CBMA can improve backscatter throughput by more than 10× in challenging indoor scenarios with obstacles and interference.

Acknowledgement

This research is partially supported by National key research and development plan 2017YFB0801702, and by the NSF China under Grants No. 61772546, 61625205, 61702011, 61632010, 61751211, 61190114, 61232018, 61232016, PAPD, CICAEET and NSF of Jiangsu For Distinguished Young Scientist: BK20150030, and in part supported by the Anhui Provincial Natural Science Foundation: 1908085QF296, 1808085QF191. Nanhuan Mi and Xiaoxue Zhang are co-primary authors. Panlong Yang, Xiang-Yang Li, and Xin He are co-corresponding authors. We also want to thank Prof. Yubo Yan at USTC for the helpful suggestions and discussions to improve the quality of this paper.

References

[1] S. Inc., "Internet of things (iot) connected devices installed base worldwide from 2015 to 2025," 2018, Accessed on 2018-08-01. [Online]. Available: ={https://www.statista.com/statistics/471264/iot-number-of-connected-devices-worldwide},

[2] D. Bharadia, K. R. Joshi, M. Kotaru, and S. Katti, "BackFi: High throughput wifi backscatter," in *Proc. of ACM SIGCOMM*. New York, NY, USA: ACM, 2015, pp. 283–296.

[3] A. Wang, V. Iyer, V. Talla, J. R. Smith, and S. Gollakota, "Fm backscatter: Enabling connected cities and smart fabrics." in *NSDI*, 2017, pp. 243–258.

[4] V. Talla, M. Hessar, B. Kellogg, A. Najafi, J. R. Smith, and S. Gollakota, "Lora backscatter: Enabling the vision of ubiquitous connectivity," *Proc. of ACM Interact. Mob. Wearable Ubiquitous Technol.*, vol. 1, no. 3, pp. 105:1–105:24, Sep. 2017.

[5] Y. Peng, L. Shangguan, Y. Hu, Y. Qian, X. Lin, X. Chen, D. Fang, and K. Jamieson, "Plora: A passive long-range data network from ambient lora transmissions," in *Proceedings of the 2018 Conference of the ACM Special Interest Group on Data Communication*. ACM, 2018, pp. 147–160.

[6] M. Hessar, A. Najafi, and S. Gollakota, "Netscatter: Enabling large-scale backscatter networks," *arXiv preprint arXiv:1808.05195*, 2018.

[7] B. G. Agee, *Solving the Near-Far Problem: Exploitation of Spatial and Spectral Diversity in Wireless Personal Communication Networks*. Boston, MA: Springer US, 1994, pp. 69–80.

[8] R. Gold, "Optimal binary sequences for spread spectrum multiplexing (corresp.)," *IEEE Transactions on Information Theory*, vol. 13, no. 4, pp. 619–621, October 1967.

[9] A. N. Parks, A. Liu, S. Gollakota, and J. R. Smith, "Turbocharging ambient backscatter communication," in *Proc. of ACM SIGCOMM*. New York, NY, USA: ACM, 2014, pp. 619–630.

[10] V. Iyer, V. Talla, B. Kellogg, S. Gollakota, and J. Smith, "Inter-technology backscatter: Towards internet connectivity for implanted devices," in *Proc. of ACM SIGCOMM*. New York, NY, USA: ACM, 2016.

[11] "Techincal description of SPDT," at:http://www.analog.com/media/en/technical-documentation/data-sheets/hmc190b.pdf.

[12] P. Zhang, D. Bharadia, K. Joshi, and S. Katti, "HitchHike: Practical backscatter using commodity wifi," in *Proc. of ACM SenSys*. New York, NY, USA: ACM, 2016.

[13] V. Liu, A. Parks, V. Talla, S. Gollakota, D. Wetherall, and J. R. Smith, "Ambient backscatter: Wireless communication out of thin air," in *Proc. of ACM SIGCOMM*. New York, NY, USA: ACM, 2013.

[14] B. Kellogg, A. Parks, S. Gollakota, J. R. Smith, and D. Wetherall, "Wi-Fi backscatter: Internet connectivity for RF-powered devices," in *Proc. of ACM SIGCOMM*. New York, NY, USA: ACM, 2014, pp. 607–618.

[15] P. Zhang and D. Ganesan, "Enabling bit-by-bit backscatter communication in severe energy harvesting environments," in *Proc. of USENIX NSDI*. Berkeley, CA, USA: USENIX Association, 2014.

[16] V. Talla, B. Kellogg, B. Ransford, S. Naderiparizi, S. Gollakota, and J. R. Smith, "Powering the next billion devices with Wi-Fi," in *Proc. of ACM CoNEXT*. New York, NY, USA: ACM, 2015.

[17] B. Kellogg, V. Talla, J. R. Smith, and S. Gollakot, "PASSIVE WI-FI: Bringing low power to Wi-Fi transmissions," in *Proc. of USENIX NSDI*, 2016.

[18] M. Jin, Y. He, X. Meng, Y. Zheng, D. Fang, and X. Chen, "FlipTracer: Practical parallel decoding for backscatter communication," in *Proc. of ACM MobiCom*. New York, NY, USA: ACM, 2017, pp. 275–287.

[19] P. Zhang, C. Josephson, D. Bharadia, and S. Katti, "FreeRider: Backscatter communication using commodity radios," in *Proc. of CoNEXT*. New York, NY, USA: ACM, 2017.

[20] T. Kim and W. Lee, "Exploiting residual channel for implicit Wi-Fi backscatter networks," in *Proc. of IEEE INFOCOM*, April 2018, pp. 1–9.

[21] C. Yang, J. Gummeson, and A. Sample, "Riding the airways: Ultra-wideband ambient backscatter via commercial broadcast systems," in *Proc. of IEEE INFOCOM*, May 2017, pp. 1–9.

[22] A. Wang, V. Iyer, V. Talla, J. R. Smith, and S. Gollakota, "FM backscatter: Enabling connected cities and smart fabrics," in *Proc. of USENIX NSDI*. Boston, MA: USENIX Association, 2017, pp. 243–258.

[23] P. Zhang, J. Gummeson, and D. Ganesan, "Blink: A high throughput link layer for backscatter communication," in *Proc. of ACM MobiSys*. New York, NY, USA: ACM, 2012, pp. 99–112.

[24] P. Hu, P. Zhang, and D. Ganesan, "Laissez-faire: Fully asymmetric backscatter communication," in *Proceedings of the 2015 ACM Conference on Special Interest Group on Data Communication*, ser. SIGCOMM '15. New York, NY, USA: ACM, 2015, pp. 255–267.

[25] "EPC UHF Gen2 Air Interface Protocol," at:https://www.gs1.org/epcrfid/epc-rfid-uhf-air-interface-protocol/2-0-1.

[26] H. Liu and J.-P. Ciou, "Performance analysis of multi-carrier RFID systems," in *Proc. of SPECTS*, vol. 41, July 2009, pp. 112–116.

[27] C. Mutti and C. Floerkemeier, "CDMA-based RFID systems in dense scenarios: Concepts and challenges," in *Proc. of IEEE RFID*, April 2008, pp. 215–222.

[28] J. Yu, K. Liu, and G. Yan, "A novel rfid anti-collision algorithm based on sdma," in *Proc. of WiCOM*, Oct 2008, pp. 1–4.

[29] D. Shen, G. Woo, D. P. Reed, A. B. Lippman, and J. Wang, "Separation of multiple passive rfid signals using software defined radio," in *Proc. of IEEE RFID*, April 2009, pp. 139–146.

[30] J. Wang, H. Hassanieh, D. Katabi, and P. Indyk, "Efficient and reliable low-power backscatter networks," in *Proc. of ACM SIGCOMM*.